CLEAN Receiver for CDMA MIMO Radar

Gaston Solodky[1], Oren Longman[1], Ishai Eljarat[1], and Igal Bilik[2]
[1]Israel Technical Center, General Motors
[2]School of Electrical and Computer Engineering, Ben-Gurion University of the Negev, Israel
E-mail: {gasti.solodky, oren.longman, ishai.eljarat}@gm.com, and bilik@bgu.ac.il

***Abstract*—Implementation of the intra-coding code-division multiple access (CDMA) multiple-input multiple-output (MIMO) radars requires orthogonality between the transmitted codewords. The lack of complete orthogonality between practical codewords induces sidelobes in the received signal which mask weak targets and increase probability of false alarm (PFA). This work proposes a novel and efficient CLEAN CDMA-MIMO approach, which considers all the transmitted codewords and the receiver noise coloring. The performance of the proposed approach is evaluated via simulations of a practical automotive scenario.**

***Index Terms*—CLEAN, Maximum Likelihood Estimation, Automotive Radar, CDMA-MIMO Radar**

I. Introduction

RECENTLY, multiple advanced active safety and autonomous driving features were introduced in consumer vehicles [1]. Conventional sensing suite consists of cameras, LIDARs and radars [2]. Automotive radars play a central role in this sensing suite, since they enable low-cost sensing, provide robustness to adverse weather and lighting conditions, achieve long operation ranges and obtain direct measurement of target's radial velocity [3]. However, the main radar's limitation, compared to cameras and LIDARs, is its relatively low angular resolution [2].

A radar's angular resolution is determined by its antenna aperture, which is limited by the vehicle platform form-factor requirements [4]. The multiple-input multiple-output (MIMO) radar approach enables higher angular resolution for a given physical antenna aperture [5]. The MIMO radar approach considers simultaneous transmission of multiple orthogonal codewords from different transmit antennas. The orthogonality between codewords is needed to distinguish the different transmitter-target-receiver channels. However, fully orthogonal signals do not exist, and only low correlated signals can be implemented [6], [7].

As part of the waveform design, multiple schemes were studied to achieve orthogonality between the MIMO radar transmissions [6]–[8]. Time-division multiple access (TDMA) is the most widely-used approach for MIMO radar transmission scheme implementation, due to its simplicity and ability to achieve high orthogonality [9]. However, TDMA implementation is inefficient in terms of transmit power. In addition, TDMA MIMO radar has tighter constraints on the maximal unambiguous Doppler achievable, which makes this approach infeasible for MIMO radars with a large number of antenna elements [1], [2], [10].

Code-division multiple access (CDMA) is an alternative approach to achieve orthogonality for MIMO radars. The CDMA-MIMO approach addresses some of the TDMA approach drawbacks at the expense of reduced orthogonality. Degradation in orthogonality increases the sidelobe level, which reduces the probability of detection (PD), and increases the probability of false alarm (PFA) [11].

This work proposes the intra-coding scheme for CDMA-MIMO radars, i.e. in the fast-time domain, which may have elevated sidelobes in the range domain [11]. In a typical urban automotive scenario, for instance, a strong static infrastructure's sidelobes may mask a static vulnerable road user (VRU). The orthogonality loss is addressed by a modified CLEAN algorithm [12], which increases the PD of the previously masked targets and reduces the PFA. CLEAN algorithm was used in [13]–[16] for clutter and sidelobes rejection. In [17] a maximum likelihood estimator (MLE) for the amplitude estimation for inverse synthetic aperture was introduced.

This work proposes a novel and computationally efficient method to implement the CLEAN receiver for CDMA-MIMO radars. The proposed CLEAN method introduces a novel MLE step for the amplitude estimation, which takes into account the different codewords and the noise coloring by the CLEAN process.

The rest of the paper is organized as follows. Section II presents the CDMA-MIMO model and the CLEAN algorithm. The proposed CLEAN receiver and the efficient CLEAN receiver are detailed in Section III, and the amplitude estimator is developed in Section IV. Performance of the proposed approach is evaluated in Section V via simulations. Our conclusions are given in Section VI.

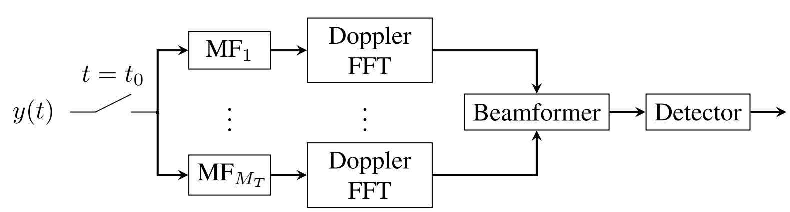

Fig. 1. A standard intra-coding CDMA-MIMO radar receiver processing for a single channel.

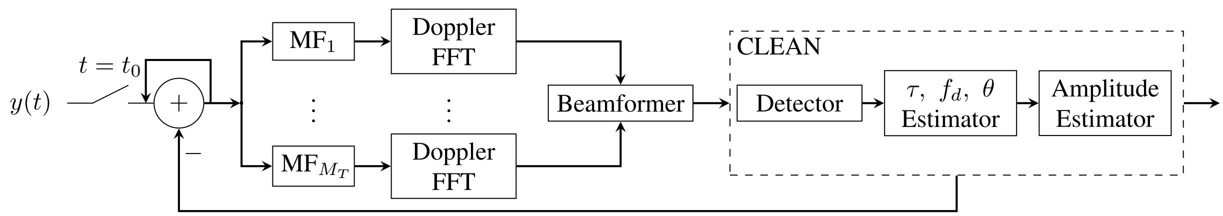

Fig. 2. An intra-coding CDMA-MIMO radar single channel processing with a conventional CLEAN.

II. Problem Definition

A. CDMA-MIMO Model

Consider a CDMA-MIMO radar with M_T transmitters and M_R receivers, where different codewords are simultaneously transmitted from different transmitters. The K transmitted chirps impinging L targets and the kth received chirp at the rth receiver is

$$y_{r_k}(t) = \sum_{l=1}^{L} A_l \sum_{m=1}^{M_T} s_{m_k}(t, \tau_l, f_{d_l}, \theta_l) + n_k(t)\ , \tag{1}$$

where $s_{m_k}(\cdot)$ is the normalized mth codeword of the kth chirp, transmitted from the mth transmitter, $A_l,\ \tau_l,\ f_{d_l}$ and θ_l are the amplitude, time delay, Doppler frequency shift and direction-of-arrival (DOA) of the lth target, respectively. $n_k(t)$ is a complex circular symmetric additive white Gaussian-distributed noise with variance σ_n^2 of the kth chirp. In the vectorial form, (1) can be rewritten as

$$\boldsymbol{y}_r(t) = \sum_{l=1}^{L} A_l \sum_{m=1}^{M} \boldsymbol{s}_m(t, \tau_l, f_{d_l}, \theta_l) + \boldsymbol{n}(t)\ , \tag{2}$$

where $\boldsymbol{y}_r(t) = [y_{r_1}(t), y_{r_2}(t), \cdots, y_{r_K}(t)]^T$, $\boldsymbol{s}_m(t) = [s_{m_1}(t), s_{m_2}(t), \cdots, s_{m_K}(t)]^T$ and $\boldsymbol{n}(t) = [n_1(t), n_2(t), \cdots, n_K(t)]^T$. The time-sampled received signal is

$$\bar{\boldsymbol{y}}_r = \sum_{l=1}^{L} A_l \boldsymbol{x}_l + \tilde{\boldsymbol{n}}\ , \tag{3}$$

where $\boldsymbol{Y} = [\boldsymbol{y}_r(t_1), \boldsymbol{y}_r(t_2), \cdots, \boldsymbol{y}_r(t_N)]^T$, $\bar{\boldsymbol{y}}_r = \mathrm{vec}(\boldsymbol{Y})$, $\boldsymbol{S}_{m_l} = [\boldsymbol{s}_m(t_1), \boldsymbol{s}_m(t_2), \cdots, \boldsymbol{s}_m(t_N)]^T$, $\tilde{\boldsymbol{s}}_{m_l} = \mathrm{vec}(\boldsymbol{S}_{m_l})$, $\boldsymbol{x}_l = \sum_{m=1}^{M} \tilde{\boldsymbol{s}}_{m_l}$, $\boldsymbol{N} = [\boldsymbol{n}(t_1), \boldsymbol{n}(t_2), \cdots, \boldsymbol{n}(t_N)]^T$, $\tilde{\boldsymbol{n}} = \mathrm{vec}(\boldsymbol{N})$ and $\mathrm{vec}(\cdot)$ is the vector operator. Considering the deterministic signal amplitude and white normally-distributed noise, the received signal in (3) is complex normal distributed, $\bar{\boldsymbol{y}}_r \sim \mathcal{CN}(\sum_{l=1}^{L} A_l \boldsymbol{x}_l, \sigma_n^2 \boldsymbol{I})$. The main radar goal is to estimate the number of targets L, the targets' amplitudes, $\{A_l\}_{l=1}^{L}$, time-of-arrival delays, $\{\tau_l\}_{l=1}^{L}$, Doppler frequencies, $\{f_{d_l}\}_{l=1}^{L}$ and DOAs, $\{\theta_l\}_{l=1}^{L}$. For better target's parameters estimation performance of the CLEAN algorithm, it is assumed, without the loss of generality, that the targets' amplitudes obey:

$$A_1 \gg A_2 \gg \cdots \gg A_L\ . \tag{4}$$

where $\gg$ means much greater than. Otherwise, a false target that is created by a constructive interference of the sidelobe responses will degrade the weak target detection quality [14].

Fig. 1 shows a standard processing flow for a single receiver CDMA-MIMO radar. The processing consists of M_T matched filters (MF), matched to transmitted codewords, Doppler fast Fourier transform (FFT), beamformer and detector.

B. CLEAN Algorithm

CLEAN is an iterative deconvolution algorithm, which assumes the presence of point-like targets [12]. According to CLEAN, the strongest target is first detected by searching for the maximal amplitude. Next, considering the signal's response of the strongest point target, X, its contribution is subtracted from the received signal

$$Y_l = Y_{l-1} - \gamma X\ , \tag{5}$$

to unveil weaker masked targets. Y_l is the response after l CLEAN steps, $l = 1, 2, \ldots, L$, Y_0 is the initial response and $0 \leq \gamma \leq 1$ is the subtraction factor. γ is chosen to be smaller than one, for the stability of the process, usually $0.1 \leq \gamma \leq 0.9$ [14]. This process is repeated iteratively until the remaining signal's peak power is below a predefined threshold, or when the maximal allowed number of iterations is achieved. Considering automotive radar operating in the far-field regime, it is reasonable to assume that the target's properties are the same for the all transmitted codewords.

III. The Proposed CLEAN CDMA-MIMO Radar

The lack of orthogonality between transmitted codewords in CDMA-MIMO radar with intra-coding scheme induces the high range-domain sidelobes in the reconstructed radar image. This phenomenon reduces the receiver's dynamic range and as a result, decreases the PD and increases the PFA.

This section introduces the proposed approach to increase orthogonality between the received CDMA-MIMO radar codewords. The main idea of the proposed receiver processing flow is to use the CLEAN algorithm. The following subsections detail the proposed approach implementation with the conventional and the innovative efficient implementation of the CLEAN.

A. CDMA-MIMO Radar with Conventional CLEAN

Successful operation of the CLEAN approach considers the efficient subtraction of the strongest target from the received signal, at each iteration. Therefore, the strongest target's amplitude, range, Doppler and DOA need to be estimated.

Fig. 2 shows the proposed single receiver processing. First, the strongest target is detected, then its range, Doppler and DOA are estimated from the range-Doppler-beam (RDB) map at the output of the beamformer. Next, the target's amplitude is estimated, and finally, the M_T transmitted codewords responses are iteratively subtracted over the iterations.

The conventional CLEAN performs the time-domain subtraction:

$$\tilde{\boldsymbol{y}}_l = \tilde{\boldsymbol{y}}_{l-1} - \gamma \hat{A}_l \hat{\boldsymbol{x}}_l\ , \tag{6}$$

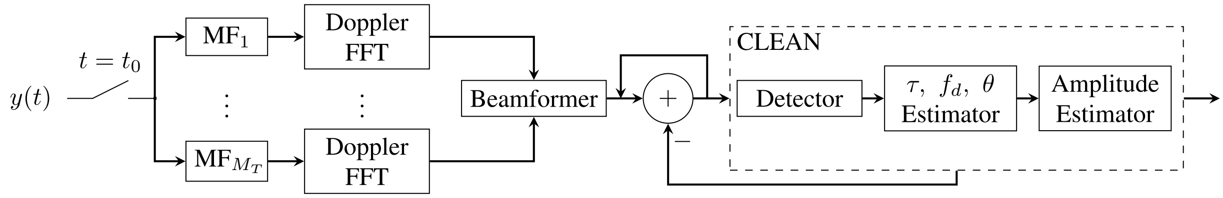

Fig. 3. An intra-coding CDMA-MIMO radar single channel processing with a computationally efficient CLEAN.

where the subtraction is element wise, $\tilde{\boldsymbol{y}}_l$ is the output of the lth CLEAN step, $\hat{A}_l$ is the estimated amplitude of the lth target and $\hat{\boldsymbol{x}}_l$ is the negative feedback signal, seen in Fig. 2, of the lth target modeled codeword

$$\hat{\boldsymbol{x}}_l = \sum_{m=1}^{M} \tilde{\boldsymbol{s}}_{m_l}(t, \hat{\tau}_l, \hat{f}_{d_l}, \hat{\theta}_l) \ . \tag{7}$$

The major drawback of the conventional CLEAN-based CDMA-MIMO radar approach is the increased computational complexity due to the CLEAN iterative process, the MFs, Doppler FFTs and beamformer need to be calculated as many times as the number of iterations. Moreover, for the MIMO radar with M_R receive channels, the CLEAN processing in Fig. 2 is replicated M_R times.

The conventional CLEAN implementation, can be easily extended to the inter-coding scheme as well, i.e. in the slow-time domain, where the MF and Doppler FFT in Fig. 2 are replaced with a range FFT and Doppler MF, respectively.

B. CDMA-MIMO Radar with Efficient CLEAN

This subsection introduces the computationally efficient implementation of the CLEAN approach for the CDMA-MIMO radar. The main idea is to perform the CLEAN stage subtraction at the output of the beamformer in the RDB domain. That is, the negative feedback signal in the efficient approach, is the processing output tensor, after the beamforming of $\hat{\boldsymbol{x}}_l$ from (7), $\hat{\boldsymbol{X}}_{\text{RDB}l}$, of size $N_R \times N_D \times N_B$ where N_R, N_D and N_B are the range, Doppler and beam sizes, respectively. Fig. 3 shows the processing of the CDMA-MIMO radar with efficient CLEAN

$$\mathbf{RDB}_l = \mathbf{RDB}_{l-1} - \gamma \hat{A}_l \hat{\boldsymbol{X}}_{\text{RDB}l} \ , \tag{8}$$

where subtraction is element-wise and $\mathbf{RDB}_l$ is the output tensor, after the beamforming of $\tilde{\boldsymbol{y}}_l$ from (7), of size $N_R \times N_D \times N_B$ of the lth CLEAN step. As a result, this implementation is more efficient, since the MF, Doppler FFT and beamformer are calculated only once per frame. However, this comes with a memory cost of storing an additional lookup table (LUT) with all the possible CDMA responses for the different transmit codewords, ranges, Doppler frequencies and DOAs.

Notice that using sufficiently large LUT, is allowing to achieve the performance of the CDMA-MIMO radar with a conventional CLEAN implementation, since the processing is linear. Alternatively, the codewords generation in the conventional approach can be implemented using a LUT as well. In addition, notice that the proposed CDMA-MIMO radar implementation with CLEAN allows to improve PD and PFA performance by unmasking weak targets, and facilitating the operation of a full MIMO scheme by increasing orthogonality between received signals, without compromising the receiver bandwidth, chirp duration and dynamic range.

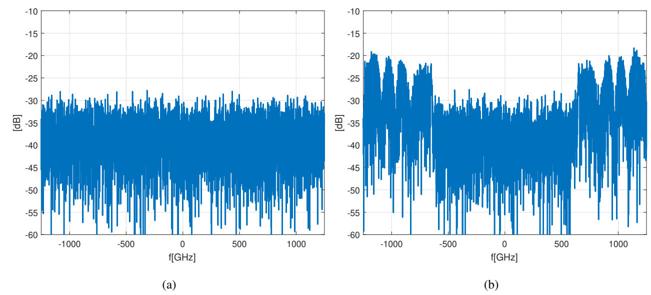

Fig. 4. Noise spectrum (a) at the input and (b) at the output of a CLEAN iteration.

To demonstrate the processing complexity improvement of the efficient approach, let's assume a scene with L different targets. In the conventional approach, the MF, Doppler FFT and beamformer need to be calculated up to L times. While in the efficient method, they are computed only once.

IV. Amplitude Estimation

The critical stage of the proposed CLEAN implementation is the amplitude estimation. This work proposes the MLE for the target's amplitude estimation.

A. Naive CLEAN Amplitude Estimator

A CLEAN amplitude estimator for radar is considered in [17]

$$\hat{a}_l = (\hat{\boldsymbol{x}}_l^H \hat{\boldsymbol{x}}_l)^{-1} \hat{\boldsymbol{x}}_l^H \tilde{\boldsymbol{y}}_{l-1} = \frac{\Re(\hat{\boldsymbol{x}}_l^H \tilde{\boldsymbol{y}}_{l-1})}{\hat{\boldsymbol{x}}_l^H \hat{\boldsymbol{x}}_l} \ , \tag{9}$$

where $\Re(\cdot)$ is the real operator, $\hat{\boldsymbol{x}}_l$ is the estimated signal from the lth target in (7) and $\tilde{\boldsymbol{y}}_{l-1}$ is the signal at the input of the $l-1$ CLEAN step.

The amplitude estimator in [17] assumes a white noise for the entire CLEAN process. However, the CLEAN process in (6) "colors" the noise, which affects the likelihood function, and the estimator statistics. Fig. 4 demonstrate this noise "coloring" effect. Subplots (a) and (b) in Fig. 4 compare the noise spectrum between the CLEAN input and output. Notice that at the output of a CLEAN iteration, the noise is colored, and therefore, the amplitude estimator in (9) from [17] is not the MLE.

B. Proposed CLEAN Amplitude MLE

This subsection introduces the proposed CLEAN amplitude MLE that considers the noise coloring effect. At the first step of CLEAN, the amplitude of the strongest target, A_1, is estimated. Since the noise at the input of the first CLEAN iteration is Gaussian, the initial input signal is normally distributed, $\tilde{\boldsymbol{y}} \sim \mathcal{CN}(\boldsymbol{\mu}_{\tilde{\boldsymbol{y}}} = \sum_{l=1}^{L} A_l \boldsymbol{x}_l, \boldsymbol{\Sigma}_{\tilde{\boldsymbol{y}}} = \sigma_n^2 \boldsymbol{I})$ and the MLE at the first step is

$$\begin{aligned} \hat{A}_1 &= \arg\max_{A_1} f(\tilde{\boldsymbol{y}}_0 | A_1) \\ &= \arg\min_{A_1} (\tilde{\boldsymbol{y}}_0 - A_1 \hat{\boldsymbol{x}}_1)^H \boldsymbol{\Sigma}_{\tilde{\boldsymbol{y}}_0}^{-1} (\tilde{\boldsymbol{y}}_0 - A_1 \hat{\boldsymbol{x}}_1) \\ &= \frac{\tilde{\boldsymbol{y}}_0^H \hat{\boldsymbol{x}}_1 + \hat{\boldsymbol{x}}_1^H \tilde{\boldsymbol{y}}_0}{2\hat{\boldsymbol{x}}_1^H \hat{\boldsymbol{x}}_1} = \frac{\Re(\hat{\boldsymbol{x}}_1^H \tilde{\boldsymbol{y}}_0)}{\hat{\boldsymbol{x}}_1^H \hat{\boldsymbol{x}}_1}, \end{aligned} \tag{10}$$

where $f(\tilde{\boldsymbol{y}}_0|A_1) = L_{A_1}$ is the conditional likelihood function, given the observation $\tilde{\boldsymbol{y}}_0$. We can see that the estimation is equivalent to (9), since at the first iteration the noise is still white. At the first CLEAN iteration, the strongest target is subtracted from the input signal

$$\tilde{\boldsymbol{y}}_1 = \tilde{\boldsymbol{y}}_0 - \gamma \hat{A}_1 \hat{\boldsymbol{x}}_1 = \tilde{\boldsymbol{y}}_0 - \gamma \frac{\Re(\hat{\boldsymbol{x}}_1^H \tilde{\boldsymbol{y}}_0)}{\hat{\boldsymbol{x}}_1^H \hat{\boldsymbol{x}}_1} \hat{\boldsymbol{x}}_1 . \tag{11}$$

Since $\tilde{\boldsymbol{y}}_1$ is a linear combination of Gaussian-distributed vectors, it is also Gaussian-distributed, and the likelihood function at the second CLEAN iteration is

$$L_{A_2} = (\tilde{\boldsymbol{y}}_1 - A_2 \hat{\boldsymbol{x}}_2)^H \boldsymbol{\Sigma}_{\tilde{\boldsymbol{y}}_1}^{-1} (\tilde{\boldsymbol{y}}_1 - A_2 \hat{\boldsymbol{x}}_2) . \tag{12}$$

The resulting amplitude estimator is

$$\hat{A}_2 = \frac{\tilde{\boldsymbol{y}}_1^H \boldsymbol{\Sigma}_{\tilde{\boldsymbol{y}}_1}^{-1} \hat{\boldsymbol{x}}_2 + \hat{\boldsymbol{x}}_2^H \boldsymbol{\Sigma}_{\tilde{\boldsymbol{y}}_1}^{-1} \tilde{\boldsymbol{y}}_1}{2\hat{\boldsymbol{x}}_2^H \boldsymbol{\Sigma}_{\tilde{\boldsymbol{y}}_1}^{-1} \hat{\boldsymbol{x}}_2} = \frac{\Re(\hat{\boldsymbol{x}}_2^H \boldsymbol{\Sigma}_{\tilde{\boldsymbol{y}}_1}^{-1} \tilde{\boldsymbol{y}}_1)}{\hat{\boldsymbol{x}}_2^H \boldsymbol{\Sigma}_{\tilde{\boldsymbol{y}}_1}^{-1} \hat{\boldsymbol{x}}_2} . \tag{13}$$

Similarly, at the lth CLEAN iteration the likelihood function is given by

$$L_{A_l} = (\tilde{\boldsymbol{y}}_{l-1} - A_l \hat{\boldsymbol{x}}_l)^H \boldsymbol{\Sigma}_{\tilde{\boldsymbol{y}}_{l-1}}^{-1} (\tilde{\boldsymbol{y}}_{l-1} - A_l \hat{\boldsymbol{x}}_l) , \tag{14}$$

and the amplitude estimator is given by

$$\hat{A}_l = \frac{\tilde{\boldsymbol{y}}_{l-1}^H \boldsymbol{\Sigma}_{\tilde{\boldsymbol{y}}_{l-1}}^{-1} \hat{\boldsymbol{x}}_l + \hat{\boldsymbol{x}}_l^H \boldsymbol{\Sigma}_{\tilde{\boldsymbol{y}}_{l-1}}^{-1} \tilde{\boldsymbol{y}}_{l-1}}{2\hat{\boldsymbol{x}}_l^H \boldsymbol{\Sigma}_{\boldsymbol{y}_{l-1}}^{-1} \hat{\boldsymbol{x}}_l} = \frac{\Re(\hat{\boldsymbol{x}}_l^H \boldsymbol{\Sigma}_{\tilde{\boldsymbol{y}}_{l-1}}^{-1} \tilde{\boldsymbol{y}}_{l-1})}{\hat{\boldsymbol{x}}_l^H \boldsymbol{\Sigma}_{\boldsymbol{y}_{l-1}}^{-1} \hat{\boldsymbol{x}}_l} . \tag{15}$$

Notice that the statistics of the signal at the CLEAN output varies over iterations, and therefore, need to be recalculated at each CLEAN iteration. The covariance matrix can be calculated via an analytic calculation or via sample covariance matrix

$$\begin{aligned} \boldsymbol{\mu}_{\tilde{\boldsymbol{y}}_l} &= \boldsymbol{\mu}_{\tilde{\boldsymbol{y}}_{l-1}} - \gamma \frac{\Re(\hat{\boldsymbol{x}}_l^H \boldsymbol{\Sigma}_{\tilde{\boldsymbol{y}}_{l-1}}^{-1} \boldsymbol{\mu}_{\tilde{\boldsymbol{y}}_{l-1}})}{\hat{\boldsymbol{x}}_l^H \boldsymbol{\Sigma}_{\tilde{\boldsymbol{y}}_{l-1}}^{-1} \hat{\boldsymbol{x}}_l} \hat{\boldsymbol{x}}_l \\ \boldsymbol{\Sigma}_{\tilde{\boldsymbol{y}}_l} &= \mathbb{E}[\tilde{\boldsymbol{y}}_l \tilde{\boldsymbol{y}}_l^H] - \boldsymbol{\mu}_{\tilde{\boldsymbol{y}}_l} \boldsymbol{\mu}_{\tilde{\boldsymbol{y}}_l}^H \end{aligned} \tag{16}$$

where,

$$\begin{aligned} \mathbb{E}[\tilde{\boldsymbol{y}}_l \tilde{\boldsymbol{y}}_l^H] = \mathbb{E}[\tilde{\boldsymbol{y}}_{l-1} \tilde{\boldsymbol{y}}_{l-1}^H] - \gamma \mathbb{E}[\tilde{\boldsymbol{y}}_{l-1} \hat{A}_l] \hat{\boldsymbol{x}}_l^H - \\ \gamma \hat{\boldsymbol{x}}_l \mathbb{E}[\hat{A}_l \tilde{\boldsymbol{y}}_{l-1}^H] + \gamma^2 \hat{\boldsymbol{x}}_l \mathbb{E}[\hat{A}_l^2] \hat{\boldsymbol{x}}_l^H \end{aligned} \tag{17}$$

and

$$\mathbb{E}[\tilde{\boldsymbol{y}}_{l-1} \hat{A}_l] = \frac{\mathbb{E}[\tilde{\boldsymbol{y}}_{l-1} \tilde{\boldsymbol{y}}_{l-1}^H] \boldsymbol{\Sigma}_{\tilde{\boldsymbol{y}}_{l-1}}^{-1} \hat{\boldsymbol{x}}_l + \mathbb{E}[\tilde{\boldsymbol{y}}_{l-1} \tilde{\boldsymbol{y}}_{l-1}^T] \boldsymbol{\Sigma}_{\tilde{\boldsymbol{y}}_{l-1}}^{-1T} \hat{\boldsymbol{x}}_l^*}{2\hat{\boldsymbol{x}}_l^H \boldsymbol{\Sigma}_{\tilde{\boldsymbol{y}}_{l-1}}^{-1} \hat{\boldsymbol{x}}_l} \tag{18}$$

TABLE I. Simulated Targets' Parameters

	Normalized Amplitude	Delay[μsec]	Doppler[m/s]
Target 1	0dB	0	0
Target 2	-16.4dB	0.022	0
Target 3	-9.1dB	0.15	0

TABLE II. CDMA-MIMO Radar Parameters

NTx	BW[MHz]	T[μsec]	α	f_c[GHz]
4	250	10	$\pm 2,\ \pm 1.92$	77

$$\begin{aligned} \mathbb{E}[\hat{A}_l^2] =& \frac{\Re(\hat{\boldsymbol{x}}_l^H \boldsymbol{\Sigma}_{\tilde{\boldsymbol{y}}_{l-1}}^{-1} \mathbb{E}[\tilde{\boldsymbol{y}}_{l-1} \tilde{\boldsymbol{y}}_{l-1}^H] \boldsymbol{\Sigma}_{\tilde{\boldsymbol{y}}_{l-1}}^{-1} \hat{\boldsymbol{x}}_l)}{2(\hat{\boldsymbol{x}}_l^H \boldsymbol{\Sigma}_{\tilde{\boldsymbol{y}}_{l-1}}^{-1} \hat{\boldsymbol{x}}_l)^2} \\ &+ \frac{\Re(\hat{\boldsymbol{x}}_l^H \boldsymbol{\Sigma}_{\tilde{\boldsymbol{y}}_{l-1}}^{-1} \mathbb{E}[\tilde{\boldsymbol{y}}_{l-1} \tilde{\boldsymbol{y}}_{l-1}^T] \boldsymbol{\Sigma}_{\tilde{\boldsymbol{y}}_{l-1}}^{-1T} \hat{\boldsymbol{x}}_l^*)}{2(\hat{\boldsymbol{x}}_l^H \boldsymbol{\Sigma}_{\tilde{\boldsymbol{y}}_{l-1}}^{-1} \hat{\boldsymbol{x}}_l)^2} \end{aligned} \tag{19}$$

and where $\hat{\boldsymbol{x}}_l^H \boldsymbol{\Sigma}_{\tilde{\boldsymbol{y}}_{l-1}}^{-1} \tilde{\boldsymbol{y}}_{l-1} = \tilde{\boldsymbol{y}}_{l-1}^T \boldsymbol{\Sigma}_{\tilde{\boldsymbol{y}}_{l-1}}^{-1T} \hat{\boldsymbol{x}}_l^*$ and $\mathbb{E}[\hat{A}_l \tilde{\boldsymbol{y}}_{l-1}^H] = \mathbb{E}[\tilde{\boldsymbol{y}}_{l-1} \hat{A}_l]^H$. The components of (17)-(19) are

$$\begin{aligned} \mathbb{E}[\tilde{\boldsymbol{y}}_l \tilde{\boldsymbol{y}}_l^T] =& \mathbb{E}[\tilde{\boldsymbol{y}}_{l-1} \tilde{\boldsymbol{y}}_{l-1}^T] - \gamma \mathbb{E}[\tilde{\boldsymbol{y}}_{l-1} \hat{A}_l] \hat{\boldsymbol{x}}_l^T - \\ & \gamma \hat{\boldsymbol{x}}_l \mathbb{E}[\hat{A}_l \tilde{\boldsymbol{y}}_{l-1}^T] + \gamma^2 \hat{\boldsymbol{x}}_l \mathbb{E}[\hat{A}_l^2] \hat{\boldsymbol{x}}_l^T, \\ \mathbb{E}[\tilde{\boldsymbol{y}}_l^* \tilde{\boldsymbol{y}}_l^H] =& \mathbb{E}[\tilde{\boldsymbol{y}}_l \tilde{\boldsymbol{y}}_l^T]^*, \\ \mathbb{E}[\tilde{\boldsymbol{y}}_l^* \tilde{\boldsymbol{y}}_l^T] =& \mathbb{E}[\tilde{\boldsymbol{y}}_l \tilde{\boldsymbol{y}}_l^H]^*, \end{aligned} \tag{20}$$

and their initial values are

$$\begin{aligned} \mathbb{E}[\tilde{\boldsymbol{y}}_0 \tilde{\boldsymbol{y}}_0^H] &= \boldsymbol{\Sigma}_{\tilde{\boldsymbol{y}}_0} + \boldsymbol{\mu}_{\tilde{\boldsymbol{y}}_0} \boldsymbol{\mu}_{\tilde{\boldsymbol{y}}_0}^H \\ &= \sigma_n^2 \boldsymbol{I} + (\sum_l A_l \hat{\boldsymbol{x}}_l)(\sum_l A_l \hat{\boldsymbol{x}}_l)^H, \\ \mathbb{E}[\tilde{\boldsymbol{y}}_0 \tilde{\boldsymbol{y}}_0^T] &= (\sum_l A_l \hat{\boldsymbol{x}}_l)(\sum_l A_l \hat{\boldsymbol{x}}_l)^T + \mathbb{E}[\boldsymbol{n}\boldsymbol{n}^T] = \boldsymbol{\mu}_{\tilde{\boldsymbol{y}}_0} \boldsymbol{\mu}_{\tilde{\boldsymbol{y}}_0}^T, \\ \mathbb{E}[\tilde{\boldsymbol{y}}_0^* \tilde{\boldsymbol{y}}_0^H] &= \mathbb{E}[\tilde{\boldsymbol{y}}_0 \tilde{\boldsymbol{y}}_0^T]^* = \boldsymbol{\mu}_{\tilde{\boldsymbol{y}}_0}^* \boldsymbol{\mu}_{\tilde{\boldsymbol{y}}_0}^H, \\ \mathbb{E}[\tilde{\boldsymbol{y}}_0^* \tilde{\boldsymbol{y}}_0^T] &= \mathbb{E}[\tilde{\boldsymbol{y}}_0 \tilde{\boldsymbol{y}}_0^H]^* = \sigma_n^2 \boldsymbol{I} + (\sum_l A_l \hat{\boldsymbol{x}}_l)^* (\sum_l A_l \hat{\boldsymbol{x}}_l)^T. \end{aligned} \tag{21}$$

First, notice that since the noise is a complex circular symmetric Gaussian vector, its pseudo covariance $\mathbb{E}[\boldsymbol{n}\boldsymbol{n}^T] = 0$ [18]. Next, notice that assuming that the target's amplitude is much stronger than all other signals (4), it is reasonable to initialize the expectation with $\mu_{y_0} \approx A_1 \hat{\boldsymbol{x}}_1$. Finally, notice that the Woodbury matrix inversion lemma can be used to calculate the matrix inversion, $\boldsymbol{\Sigma}_{\tilde{\boldsymbol{y}}_l}^{-1}$ [19].

V. Performance Evaluation

The performance of the proposed CLEAN CDMA-MIMO radar is evaluated in this section in a relevant practical automotive scenario with three static targets. In this scenario the increase in PFA and the decrease in PD, which is caused by weak target masking, is simulated. Table I summarises targets' parameters and Table II summarises the parameters of the simulated CDMA-MIMO radar with 4 transmitters and a single receiver. The Tansec coding family is considered, with codewords selected by the the ACCFG method from [11], [20].

Fig. 5 shows the output of the MF of the considered CDMA-MIMO radar with a fixed threshold in the simulated three-target scenario. Notice that the sidelobes of the strongest target mask the weakest target and the remaining target amplitude is at the level of the strongest target sidelobes approx. -11dB.

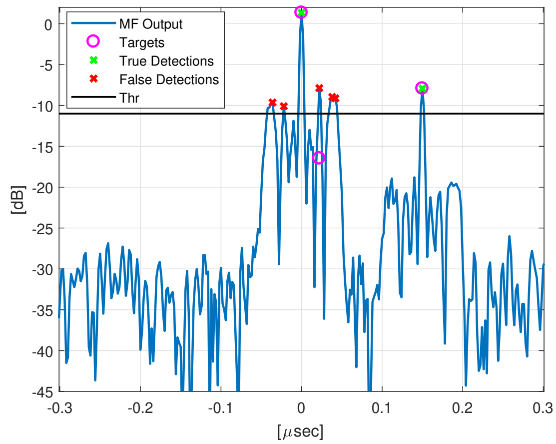

Fig. 5. CDMA-MIMO radar MF output in the three-target scenario and a fixed threshold.

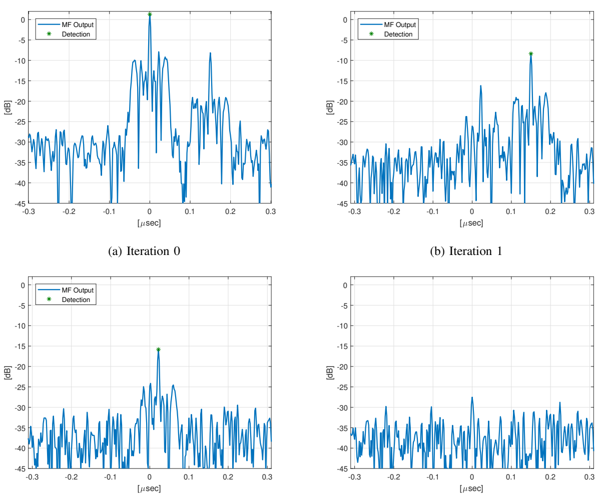

(a) Iteration 0

(b) Iteration 1

(c) Iteration 2

(d) Iteration 3

Fig. 6. The received signal after matched filter for different iteration steps.

As a result, the fixed threshold detector detects two true targets (along with additional false detections induced by the strongest target's sidelobes). In addition, notice that the weakest target was not detected. The targets' amplitudes in Fig. 5 are stronger than it appears in Table I, since the codewords are not completely orthogonal. The cross-codewords add a noise floor of ~ 1.5dB per target.

Fig. 6 shows the output of the CLEAN in the proposed CDMA-MIMO radar over CLEAN iterations. At each step the strongest peak is detected, marked by the green asterisk, its parameters are estimated and its response is subtracted. Fig. 6 shows that the proposed CDMA-MIMO radar with efficient CLEAN succeed to detected all three targets, without any false alarms.

VI. Conclusions

This work proposed a novel and efficient modified CLEAN-based detector for CDMA-MIMO radars. The proposed approach considers all the transmitted codewords and addresses the noise coloring. The proposed approach is computationally efficient. The performance of the proposed efficient CLEAN CDMA-MIMO radar was evaluated via simulations of a practical automotive scenario, demonstrating its ability to detect weak targets which are conventionally masked by the strong target sidelobes.

References

[1] S. Sun, A. P. Petropulu, and H. V. Poor, "MIMO radar for advanced driver-assistance systems and autonomous driving: Advantages and challenges," *IEEE Signal Processing Magazine*, vol. 37, no. 4, pp. 98–117, 2020.

[2] I. Bilik, O. Longman, S. Villeval, and J. Tabrikian, "The rise of radar for autonomous vehicles: Signal processing solutions and future research directions," *IEEE Signal Processing Magazine*, vol. 36, no. 5, pp. 20–31, 2019.

[3] S. M. Patole, M. Torlak, D. Wang, and M. Ali, "Automotive radars: A review of signal processing techniques," *IEEE Signal Processing Magazine*, vol. 34, no. 2, pp. 22–35, 2017.

[4] M. Murad, I. Bilik, M. Friesen, J. Nickolaou, J. Salinger, K. Geary, and J. Colburn, "Requirements for next generation automotive radars," in *IEEE Radar Conference*, pp. 1–6, 2013.

[5] J. Li and P. Stoica, "MIMO radar with colocated antennas," *IEEE Signal Processing Magazine*, vol. 24, no. 5, pp. 106–114, 2007.

[6] J. De Wit, W. Van Rossum, and A. De Jong, "Orthogonal waveforms for FMCW MIMO radar," in *IEEE Radar Conference (RADAR)*, pp. 686–691, May 2011.

[7] H. Sun, F. Brigui, and M. Lesturgie, "Analysis and comparison of MIMO radar waveforms," in *International Radar Conference*, pp. 1–6, Oct 2014.

[8] I. Eljarat, J. Tabrikian, and I. Bilik, "Collaborative spectrum allocation and waveform design for radar coexistence," in *2020 IEEE 11th Sensor Array and Multichannel Signal Processing Workshop (SAM)*, pp. 1–5, 2020.

[9] I. Bilik, S. Villeval, D. Brodeski, H. Ringel, O. Longman, P. Goswami, C. Y. Kumar, S. Rao, P. Swami, A. Jain, *et al.*, "Automotive multi-mode cascaded radar data processing embedded system," in *IEEE Radar Conference*, pp. 0372–0376, 2018.

[10] I. Shapir, I. Bilik, and G. Barkan, "Doppler ambiguity resolving in TDMA automotive MIMO radar via digital multiple PRF," in *IEEE Radar Conference*, pp. 0175–0180, 2018.

[11] G. Solodky, O. Longman, S. Villeval, and I. Bilik, "CDMA-MIMO radar with the tansec waveform," *IEEE Transactions on Aerospace and Electronic Systems*, vol. 57, no. 1, pp. 76–89, 2021.

[12] J. Högbom, "Aperture synthesis with a non-regular distribution of interferometer baselines," *Astronomy and Astrophysics Supplement Series*, vol. 15, p. 417, 1974.

[13] J. Tsao and B. D. Steinberg, "Reduction of sidelobe and speckle artifacts in microwave imaging: The CLEAN technique," *IEEE Transactions on Antennas and Propagation*, vol. 36, no. 4, pp. 543–556, 1988.

[14] R. Bose, A. Freedman, and B. D. Steinberg, "Sequence CLEAN: A modified deconvolution technique for microwave images of contiguous targets," *IEEE Transactions on Aerospace and Electronic Systems*, vol. 38, no. 1, pp. 89–97, 2002.

[15] R. Bose, "Lean CLEAN: Deconvolution algorithm for radar imaging of contiguous targets," *IEEE Transactions on Aerospace and Electronic Systems*, vol. 47, no. 3, pp. 2190–2199, 2011.

[16] K. Kulpa, M. Baczyk, M. Malanowski, J. Misiurewicz, K. Jedrzejewski, Z. Gajo, and Ł. Maslikowski, "CLEAN removal of ground clutter in mobile passive radar," in *IEEE Radar Conference*, pp. 1–4, 2019.

[17] C. Ma, T. S. Yeo, C. S. Tan, and H. S. Tan, "Sparse array 3-d isar imaging based on maximum likelihood estimation and CLEAN technique," *IEEE Transactions on Image Processing*, vol. 19, no. 8, pp. 2127–2142, 2010.

[18] R. G. Gallager, "Circularly-symmetric gaussian random vectors," *preprint*, pp. 1–9, 2008.

[19] M. A. Woodbury, "Inverting modified matrices," *Memorandum report*, vol. 42, no. 106, p. 336, 1950.

[20] O. Longman, G. Solodky, and I. Bilik, "Beam squint correction for phased array antennas using the tansec waveform," in *IEEE International Radar Conference (RADAR)*, pp. 489–493, 2020.